Pellicular Morphing Surfaces for Soft Robots

Krishna Manaswi Digumarti[1], Andrew T. Conn[1,2], and Jonathan Rossiter[1,3]

***Abstract*—Soft structures in nature endow organisms across scales with the ability to drastically deform their bodies and exhibit complex behaviours while overcoming challenges in their environments. Inspired by microstructures found in the cell membranes of the *Euglena* family of microorganisms, which exhibit giant changes in shape during their characteristic euglenoid movement, this paper presents the design, fabrication and characterisation of bio-inspired deforming surfaces. The result is a surface of interconnected strips, that deforms in 2D and 3D due to simple shear between adjacent members. We fabricate flexible polymeric strips and demonstrate three different shapes arising out of the same actuation by imposing various constraints. We characterise the strips in terms of the force required to separate them and show that the bio-inspired cross section of these strips enables them to hold up to 8N of force with a meagre 0.5mm of material thickness, while still being flexible to deform. Further, the design of a soft robot module, with an actively deformable surface has been presented which replicates the mechanism of shape change seen in the *Euglena*. This work shows the potential for this new form of shape morphing surface in realising biomimetic soft robots exhibiting large changes in shape.**

***Index Terms*—Soft Robot Materials and Design, Biologically-Inspired Robots, Flexible Robots, Mechanism Design**

I. INTRODUCTION

ORGANISMS in nature employ soft active structures in the mechanical construction of their bodies due to the many advantages offered such as the ability to deform, conform and gain entry to small apertures [1]. These soft-material components enable organisms to adapt and overcome challenges in their complex natural environments such as object manipulation and locomotion. Furthermore, such structures can be found across a wide range of scales. For example, invertebrates like cephalopods are able to deform their bodies to fit into extremely small spaces and manipulate objects [2]. On the other end of the scale are bacteria and algae that also use large deformations of their bodies for feeding, negotiating their habitat [3] and to evade predators [4]. In the context of robotics, this ability to drastically alter the shape of the body is particularly attractive when traversing through clutter or squeezing through tight spaces. Scenarios such as invasive medical procedures, inspection of pipelines and searching through collapsed rubble for survivors could potentially benefit from shape changing structures. Inspired by the actively deforming cell surface of the *Euglena* family of micro-organisms, we present the design of a novel shape changing structure based on shearing of interconnected strips and demonstrate its potential to produce giant changes in shape. Replicating pellicular sliding is a novel approach to the design of highly deformable robots, which typically employ hyperelastic materials that stretch, or folding structures such as origami.

Manuscript received: September, 09, 2018; Revised December, 29, 2018; Accepted February, 05, 2019.

This paper was recommended for publication by Kyu-Jin Cho upon evaluation of the Associate Editor and Reviewers' comments.

This work was supported by the EPSRC Centre for Doctoral Training in Future Autonomous and Robotic Systems (FARSCOPE, grant EP/L015293/1) at the Bristol Robotics Laboratory where KMD is a PhD student. AC was supported by EPSRC grant EP/P025846/1. JR was supported by EPSRC grants EP/M020460/1 and EP/M026388/1 and was also funded by the Royal Academy of Engineering as a Chair in Emerging Technologies.

Data access: Data recorded during experiments is available at University of Bristol data repository, data.bris, at https://doi.org/10.5523/bris.10.5523/bris.3v1g56bpl17bz265381d19thsm.

[1] K.M. Digumarti, A. T. Conn and J. Rossiter are with the Soft-Lab, Bristol Robotics Laboratory, BS16 1QY, Bristol, UK. (email: km.digumarti@bristol.ac.uk)

[2]A. T. Conn is also with the Department of Mechanical Engineering, University of Bristol, BS8 1TR, UK

[3]J. Rossiter is also with the Department of Engineering Mathematics, University of Bristol, BS8 1UB, UK

Digital Object Identifier (DOI): see top of this page.

A. Bioinspiration from the Euglenoid Pellicle

The inspiration for this study comes from unicellular micro-organisms called euglenoids that are found in aquatic environments. These cells are equipped with one or more flagella (fig. 1a) which the organism uses to swim rapidly. However, under certain circumstances, a slower, characteristic type of locomotion called euglenoid movement is observed in which the cell exhibits a giant change in shape (fig. 1c). Cells have been observed to transfrom from a slender elongated form to a rounded spherical form [5], displaying a change in length of 37% and radius up to 100%.

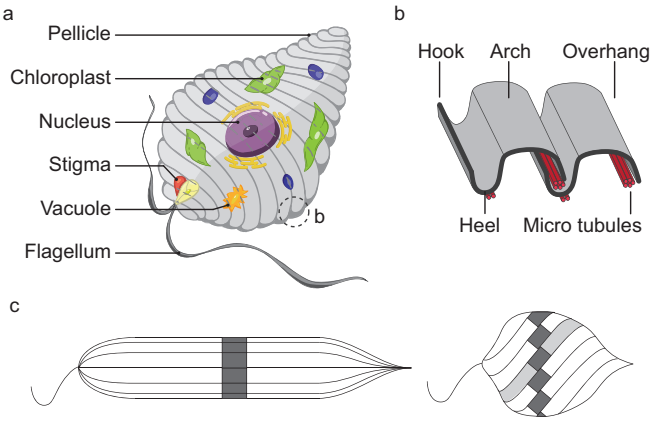

Fig. 1. (a) Schematic of a euglenoid showing various organelles and the strip-covered surface (pellicle). (b) Illustration of the pellicle showing the key elements that make up the ridges and grooves. (c) Change in shape due to sliding of strips in the pellicle (adapted from [6]).

It has been shown that these changes in shape are generated at the surface [5] due to the sliding of proteinaceous strips,

collectively called the pellicle (fig. 1b). This sliding can be described as in-plane, equi-area shear (fig. 1c) wherein the length and width of each strip remains constant but the strips freely slide against each other, keeping the total surface area constant [7].

In previous work [8], we presented the design of a hyper-elastic bellows (HEB) actuator in a soft robot to replicate the giant changes in shape of euglenoids. However, the change in shape was brought about by a mechanism different to that in the organism, as it relied on folding and elastic extension of a cylindrical bellows to change shape. In this paper, the focus is on replicating the fundamental mechanism that drives shape change in the euglenoids, namely sliding of strips in the pellicle.

The structure of the pellicle and its movement has been extensively studied [5-6, 9-14]. The cross section of each strip (fig. 1b) consists of four key elements: an arch, a heel, a hook and an overhang. The hook of one strip interlocks with the overhang of its neighbouring strip. The sliding of strips is actuated by molecular motors in the micro-tubules that are present in the region of overlap. Several shapes for the cross section have been observed [12], but we focus on the S-shaped structure (fig. 4).

B. Biomimetic Soft Actuation

Measurements of landmark features on the cell allowed for a mathematical description of the shape of the pellicle [6]. Recently, a model that treats the pellicle as a continuum was presented [13] where the kinematics of shape change are described in terms of simple shear of the strips. We use this model as a guide for the choice of actuator mechanism for the soft robot. The shear between strips is estimated to be a maximum of 8% of the length of the strip (fig. 2), which makes it a very attractive candidate for bio-inspiration. It should be noted that our interest is in generating a local shear at a specific region on the strip, which would require an actuator capable of producing much larger strains per unit length [≈25-30%]. Based on these observations, a few prominent soft robotic actuator technologies are reviewed here that could be used to generate sliding.

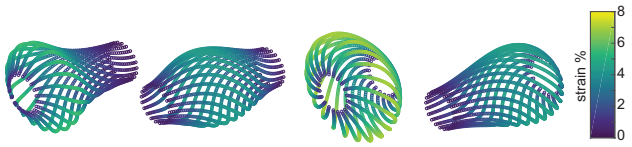

Fig. 2. Shear between strips for various input shapes (based on [13]).

Ionic polymer metal composites (IPMCs) have been used to construct multi-segmented artificial cilia [15]. Multiple sets of these actuators could be used between the strips to mimic the motion of comb like structures found in the euglenoid pellicle [12], thus enabling sliding. However, the small forces produced make them less appealing at the scale required. Ultrasonic motors have been fabricated by bonding polymers to piezoelectric materials [16] and could drive motion between the strips. Another approach could be to generate movement through the use of travelling waves, such as through soft, active materials like dielectric elastomers [17]. Large strains have been reported in the literature [18] but the requirement for relatively high actuation voltages limits the applicability of the robot.

In this work, we use coiled shape memory alloy actuators [19], [20] to achieve relative motion between adjacent strips. These actuators have been shown to generate the large strains that are suitable for the task. In addition, they can conform to the changing shape of the strips such that the force is more or less directed along the length of the strips even in a deformed configuration. Exploiting these benefits and the relative ease of control of these actuators, we present the design, fabrication and actuation of bio-inspired pellicle strips and use them in a soft robot module that is able to actively deform its surface. The novelty of our design and advantage over traditional tendon driven continuum robots is that the actuation is localised. This enables a more continuous deformation of the structure and thus a much wider range of robot deformations. In addition, we show novelty in the replication of a microscopic structure at the centimetre scale while retaining its functionality.

II. PRINCIPLE OF OPERATION

The deformation of the euglenoid cell is due to localised sliding between pellicle strips (fig. 1c). This behaviour is easy to comprehend when the shape of an interlocked pair of actuated polymeric strips is observed (fig. 3). The length of the strips is constant and since the strips do not separate from each other (fig. 4b), so is the distance between them. A local shear is generated by contraction in length of a coiled shape memory alloy (SMA) actuator that connects to points on either strip (A and B in fig. 3). In a constraint free case, the contraction of the actuator results in the sliding of one strip relative to the other (fig. 3a). When the strips are fixed to each other at one end (using adhesive), shortening of the SMA actuator results in a C-shaped curving the strips (fig. 3b). Sliding is observed only at the free end. When both ends are fixed, the strips take on an S-shape upon actuation (fig. 3c). Multiple actuated strips connected to each other can thus create a complex shape-morphing surface.

III. METHODS

A. Fabrication

The flexible strips used in this study were fabricated by extruding thermoplastic polyurethane (Desmopan 2786A [21]) in a filament extruder (Noztek Pro). A custom die was fabricated using wire electrical discharge machining (wire EDM), giving the S-shaped cross-section with a material thickness of 0.5mm throughout (fig. 4). The extruded strips were then cut down to the required length using a surgical scalpel.

Unlike 3D printable plastics such PLA and ABS which lack flexibility (elasticity modulus, E $\sim$ 1GPa), the chosen thermoplastic polyurethane can deform into the required shape (fig. 2) while being rigid enough to hold the new shape (E $\sim$ 1MPa). Elastomers commonly used in soft robots such as silicones (DragonSkin, Ecoflex, etc.) are too flexible and

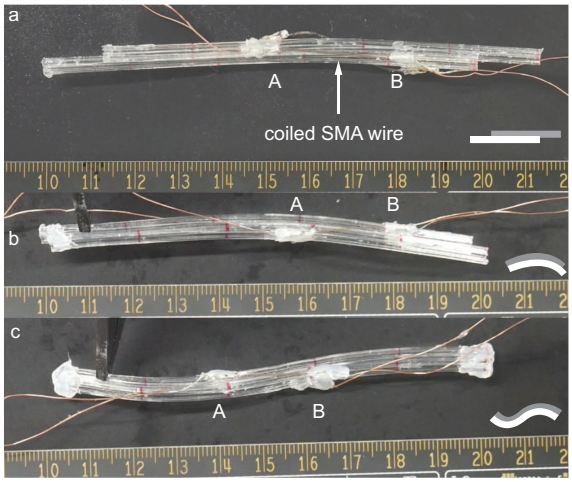

Fig. 3. Three distinct behaviours observed in two pellicle strips based on constraints imposed upon the ends. (a) With no end constraints, the strips slide against each other. (b) When one end is fixed, the strips bend to form a C-shape. Sliding is observed at the free end. (c) When both ends are fixed, an S-shaped curve is observed.

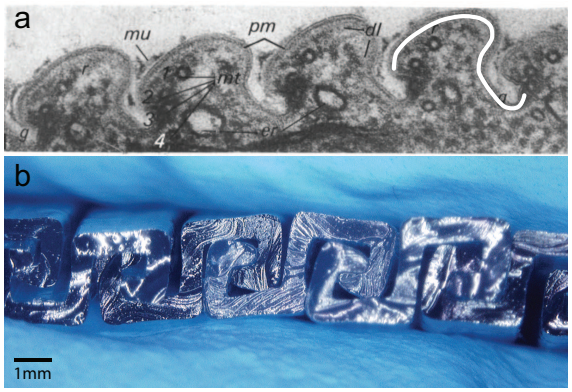

Fig. 4. (a) Cross section of the pellicle in *Euglena gracilis* [22] (reproduced with permission). One of the strips has been highlighted in white. (b) Microscopic image of the cross section of the bio-inspired polyurethane strips.

readily deform (E $\sim$ 0.01MPa). Additionally, the elasticity of the polyurethane can be easily tuned using additives. Ease of extrusion at the small scale was another reason for its choice.

Actuated strips were fabricated by attaching coiled shape memory alloy wire (BMX150, Toki Corporation, contraction of 200% of length) at two points on a pair of strips. A flexible sheet can be formed by interlocking multiple individual strips, which can bend and twist about both planar axes (see video[1]). The cylindrical structure presented in this work consists of 20 strips (compared to approx. 40 in the case of euglenoids). A flat sheet was first constructed. Actuators were then placed at the desired locations and the sheet was rolled into a cylinder. The flat ends of the cylinder were then sealed using silicone adhesive (Sil-Poxy, Smooth-On) to impose a fixed end constraint on the strips.

[1]https://youtu.be/YuP3G9eJxUA

B. Measurement of Separating Force

Three sets of experiments were conducted (fig. 5) to measure the force required to separate a pair of interlocked strips. Half strips of length 3cm were affixed to plastic attachments using high-strength epoxy adhesive (RS, Components UK, 159-3957). These acted as the clamps that pulled the strips apart. Two interlocked strips of length 10cm were held in the clamps with glue. In the first experiment, the strips were held at the end while in the second, they were held in the middle (fig. 5a and b respectively). The direction of loading is in the plane of the strips and perpendicular to the direction of sliding. This represents a component that contributes to the circumferential load on the strips of a euglenoid. The third experiment was set up in a manner loosely based on the T-peel test as defined in the ASTM-F88 standard. The two interlocked strips were peeled at one end and bent at 90 degrees (fig. 5c). They were then affixed to clamps. The peeled ends were pulled apart and the force required to peel was measured. This experiment replicates the case of radial load in the euglenoids.

In all the experiments, the clamps were pulled apart using a linear stage at a constant rate of 0.45 mm/s. Force was measured using a load cell. Displacement of one of the clamps was measured using a laser displacement sensor (LK-G152 and LKGD500, Keyence). Both force and displacement readings were recorded (USB-6001, National instruments) at a frequency of 1000Hz. Each experiment was repeated 10 times.

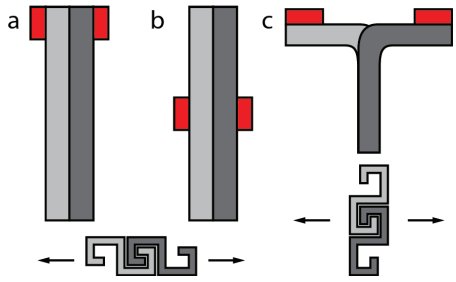

Fig. 5. Peeling test setup. (a) End separation. (b) Mid-point Separation. (c) T-peel.

C. FEA of peeling

A 2D finite element analysis of the peeling of strips was performed in addition to the experiments to predict potential regions of failure for a given cross section. One half of the S-shaped cross section was modelled in ANSYS. The two strips were defined as individual bodies that interlock with each other but do not touch initially. One of the strips was fixed while a displacement was applied to the other in the direction that causes them to separate. The contact regions between the bodies were modelled as frictionless. The material model was based on tensile test data (DIN 53504) from the manufacturer's datasheet. Distribution of stress across the cross section shows that the points of likely failure are the internal corners (regions marked in fig. 6). The deformed shape closely resembles that which was observed during experiments (fig. 7).

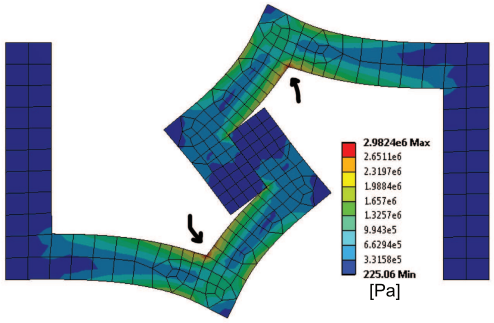

Fig. 6. Equivalent (von-Mises) stress in the strips as predicted in a finite element analysis of separation of interlocked strips. The analysis predicts material failure at the internal corners (marked with arrows).

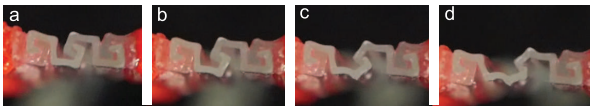

Fig. 7. Various instances during the separation of interlocked strips. (a) Initial contact. (b-c) Intermediate instances. (d) Instance prior to separation.

D. Shape Exploration

As described in sec. II, the shape of the actuated strips varies with the type of constraints imposed at the ends. To investigate this behaviour, shear strain was applied to a pair of interlocked strips at different locations and under the two constraints (fixed-free and fixed-fixed). The amount of strain was varied by changing the length of the SMA actuator used (20mm, 30mm and 40mm prior to actuation, 250mA current). Two actuators were used on either side of the pair (both aligned in the same orientation) to ensure negligible out-of-plane deformations. An antagonistic arrangement was not necessary as the inherent elasticity of the material of the strips, restored the shape to the initial configuration upon deactivation of the actuator. The location of actuation was varied by changing the points at which the actuators were affixed to each of the strips. In all, 10 different configurations were explored (fig. 10).

E. Deformation of a Pellicular Sheet

In addition to exploring shapes of pairs of strips, the passive deformation of a cylindrical sheet was also analysed. A sheet with 20 strips, each 100mm in length, was fabricated. An external load was applied in the form of a force and twist about the axis. Sliding of markers on two adjacent strips was recorded. This was compared to that predicted by the continuum model [13].

In addition to observing passive deformation, a simple soft robotic module with an actively deforming surface was fabricated. A total of 10 pairs of actuated strips of length 100mm were used. The length of the SMA actuator was 30mm and it was positioned central to the length on each pair. All the actuators were connected together to form a parallel circuit. Change in shape of the robot upon actuation was observed.

IV. RESULTS

A. Force of Separation

The force required to separate a pair of interlocked strips along a direction perpendicular to the length of the strips and in the plane of the strips is shown in fig. 8. In the case of peeling at the end (fig. 5a), separation happened at a force of 5.6±0.8N whereas in the case of peeling from the middle (fig. 5b), the force of separation was 7.9±0.4N. In both the cases, the relation between measured force and displacement was observed to be linear. The slightly larger force in the case of peeling from the middle could be attributed to distribution of force over a comparatively larger area.

The force of separation for the case of T-peel (fig. 5c) is shown in fig. 9. It was observed that the strips do not separate continuously but in stages of easy separation (force drop) followed by resistance to parting (force rise). On the onset of peeling, the strips separate partially but are held together at points further down the length (see illustrations A, B and C in fig. 9). As seen from the highlighted data, the force curve shows multiple peaks, each of which corresponds to instances at which stiction was overcome at these points and local separation occurred. The force of separation in this case is 0.14±0.02N (mean of all peaks). The variation in data between experiments could be attributed to minor imperfections on the surface of the test specimen.

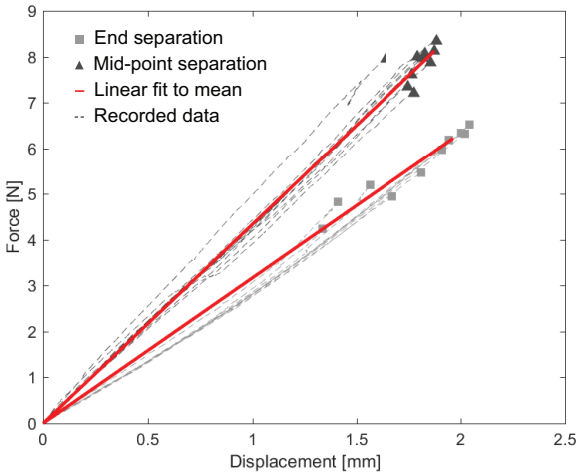

Fig. 8. Force to separate interlocked strips when peeled from the end (fig. 5a) and the middle (fig. 5b). The dotted lines indicate recorded data. End points correspond to instances of separation. The solid line is a linear fit to the mean.

B. Shape Exploration

In the cases with a fixed-free constraint imposed on the strips, upon applying a shear strain, the curve took on a C-shape. The curvature of the curve has only one local extremum. As the position of the actuator was moved from one end to the other, so did the extremum (diamond markers in fig. 10). Applying a larger strain moved this point closer to the centre of the actuator. In the cases with a fixed constraint on both ends, an S-shaped curve was observed with two local extrema

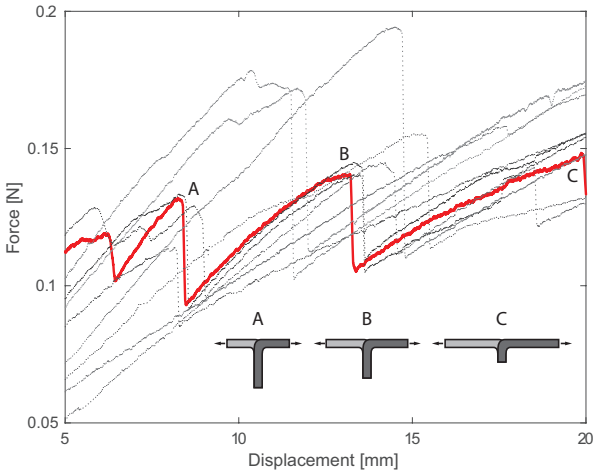

Fig. 9. Force to separate interlocked strips in the T-peel test (fig. 5c). The dotted lines indicate recorded data. The solid line highlights data from one of the experiments. Each peak (A, B, C) corresponds to the instance when separation occurred locally but the strips held together further down the length (illustrations A, B, C).

of curvature. Larger strains caused these points to lie within the bounds of the actuator while smaller strains caused either one or both the points to appear outside the bounds of the actuator. No significant change in the magnitude of absolute curvature was observed.

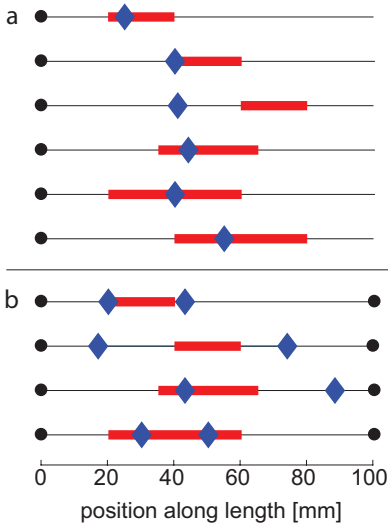

Fig. 10. Location of extrema of curvature (diamonds) as observed for different end constraints (circle indicates a fixed constraint) and different actuator lengths (thick line). (a) Fixed-free constraint. (b) Fixed-fixed constraint.

C. Deformation of Pellicular Sheet

The passive deformation of a cylindrical sheet of strips under the influence of an external load is shown in fig. 11. Sliding of strips to accommodate for the change in shape can be clearly seen through the movement of markers (placed at 5mm intervals) on adjacent strips. A maximum local strain of 2.5mm was observed in the central region which is comparable to that predicted by the model (fig. 11c).

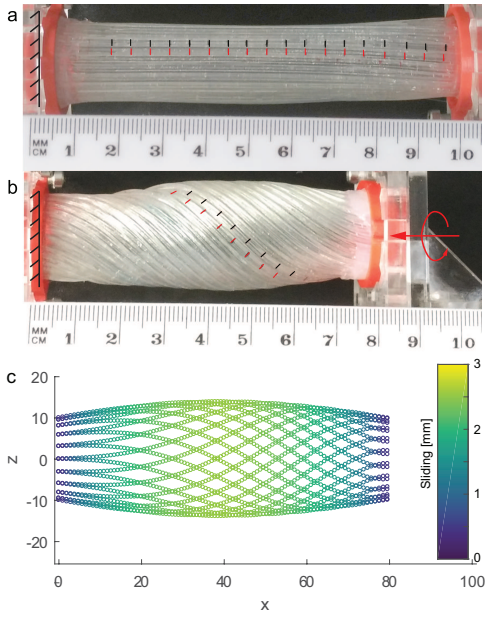

Fig. 11. Sliding of strips during change in shape is seen through the movement of markers (placed at 5mm intervals) in the (a) undeformed and (b) deformed configuration. The amount of sliding (2.5mm) is comparable to that predicted by (c) the model [13].

Active sliding and twisting of strips was observed in a cylindrical arrangement of strips. In the initial configuration with no actuation (fig. 12a), the strips are parallel to the cylinder axis. In the deformed configuration after actuation (fig. 12b), the strips slide and twist, making a 4.5° with the axis. Note that all actuators are part of the surface itself.

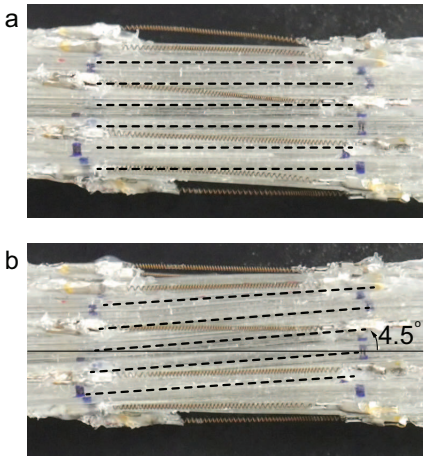

Fig. 12. Dotted lines showing the orientation of strips in the (a) initial and (b) actuated configurations.

V. DISCUSSION

In the case of a robot constructed out of the bio-inspired flexible pellicle strips, a measure that predicts failure of the surface is desirable. Experimentally determined values for

the forces of separation provide this information. The linear relation between force and displacement separation tests (fig. 8) makes it easy to model. Results from peel tests (fig. 9) indicate that failure does not instantaneously rip the entire surface apart but only causes a local separation, and peeling is discontinuous.

A second observation during tests was that the artificial pellicle surface is easy to repair. In traditional robot designs that use a monolithic skin, a failure requires the entire skin to be changed or patched using a suitable filler. For example, in the case of pneumatic networks [23], a punctured shell would have to be repaired using adhesive, which affects the performance of the system due to altering of material properties. Another example is the case of robots using dielectric elastomers [24], where the entire membrane has to be replaced. In contrast, the strip-based pellicle surface presented here is easy to repair, does not require additional material and does not require a complete replacement. A separation of strips can simply be fixed by bringing the strips together and clicking them into place (see video). Additionally, the sliding of strips is a simple shear deformation and hence there is negligible stretching or compression of material perpendicular to the direction of the strips.

The proposed actively deformable sheet is a step towards achieving euglenoid movement in a robot. However, we believe that other forms of locomotion, driven by shape change, such as terrestrial crawling, movement through granular media and traversal through a pipe are also realisable.

VI. CONCLUSIONS

In this paper, we have shown how a microscopic mechanism found in the Euglena unicellular organism can be replicated at a larger scale. We fabricated bio-inspired flexible pellicle strips to be used in the construction of soft robots that can both actively and passively change shape. We demonstrated three different behaviours (sliding, C-shape bending and S-shape bending) arising out of the same actuation mechanism on an interlocked pair of strips, by simply changing the imposed constraints. We also explored shapes arising out of varied strains imposed at different locations along the length of the strips. In addition, we demonstrated active shape change in a soft robotic module.

In the work presented here, we have only considered shapes arising from a single actuator on each pair of strips. Scaling to multiple actuators and maintaining their orientation would be a challenge. Actuation mechanisms other than SMAs are being explored, in part due to this limitation. Alternative materials such as shape memory polymers and polymer blends with tunable stiffness are being investigated. Integrating a material model on top of the kinematic model [13] is being considered.

We believe that making a completely untethered robot is achievable. More complex and asymmetric shapes are also being considered which would require individual control of each actuator.

REFERENCES

[1] S. Kim, C. Laschi, and B. Trimmer, Soft robotics: A bioinspired evolution in robotics," Trends in Biotechnology, vol. 31, no. 5, pp. 287-294, 2013.

[2] T. Hunt. "Ozy's record jar-opening skills." http://www.stuff.co.nz/marlborough-express/news/nationalnews/ 9603939/Ozys-record-jar-opening-skills. Accessed: 10.09.16.

[3] K. J. Mealand, "Mikroskopisk pacman." https://www.usn.no/forskning/forskningsnytt/mikroskopisk-pacman-article194412-27233.html. First Published: 28.06.16. Accessed: 08.03.18.

[4] Busch, A. and Hess, S., 2017. Euglenoid Movement: An Avoidance Strategy Against Algivores?. Phycologia, 56(4), p.26.

[5] T. Suzaki and R. Williamson, Euglenoid movement in euglena fusca: evidence for sliding between pellicular strips, Protoplasma, vol. 124, no. 1-2, pp. 137–146, 1985.

[6] T. Suzaki and R. E. Williamson, Cell surface displacement during euglenoid movement and its computer simulation, Cytoskeleton, vol. 6, no. 2, pp. 186–192, 1986.

[7] J. Dumais, Modes of deformation of walled cells, Journal of Experimental Botany, vol. 64, no. 15, pp. 4684-4695, 2013.

[8] K. M. Digumarti, A. T. Conn, and J. Rossiter, Euglenoid-inspired giant shape change for highly deformable soft robots, IEEE Robotics and Automation Letters, vol. 2, no. 4, pp. 2302-2307, 2017.

[9] G. Leedale, Pellicle structure in Euglena, British Phycological Bulletin, vol. 2, no. 5, pp. 291-306, 1964.

[10] H. Silverman and R. S. Hikida, Pellicle complex of Euglena gracilis: Characterization by disruptive treatments, Protoplasma, vol. 87, no. 1-3, pp. 237-252, 1976.

[11] B. S. Leander and M. A. Farmer, Comparative morphology of the euglenid pellicle. I. Patterns of strips and pores. The Journal of eukaryotic microbiology, vol. 47, no. 5, pp. 469-479, 2000.

[12] B. S. Leander and M. A. Farmer, Comparative morphology of the euglenid pellicle. ii. diversity of strip substructure, Journal of Eukaryotic Microbiology, vol. 48, no. 2, pp. 202-217, 2001.

[13] M. Arroyo, L. Heltai, D. Millan, and A. DeSimone, "Reverse engineering the euglenoid movement," Proceedings of the National Academy of Sciences, vol. 109, no. 44, pp. 17874–17879, 2012.

[14] M. Arroyo and A. DeSimone, Shape control of active surfaces inspired by the movement of euglenids, Journal of the Mechanics and Physics of Solids, vol. 62, pp. 99–112, 2014.

[15] S. Sareh, J. Rossiter, A. Conn, K. Drescher, and R. E. Goldstein, Swimming like algae: biomimetic soft artificial cilia. Journal of the Royal Society, Interface, the Royal Society, vol. 10, no. 78, 2012.

[16] J. Wu, Y. Mizuno, M. Tabaru, and K. Nakamura, Ultrasonic Motors With Polymer-Based Vibrators, vol. 62, no. 12, pp. 2169-2178, 2015.

[17] A. D. Poole, J. D. Booker, C. L. Wishart, N. McNeill, and P. H. Mellor, Performance of a prototype traveling-wave actuator made from a dielectric elastomer, IEEE/ASME Transactions on Mechatronics, vol. 17, no. 3, pp. 525-533, 2012.

[18] R. Pelrine, R. Kornbluh, Q. Pei, and J. Joseph, High-speed electrically actuated elastomers with strain greater than 100% Science, vol. 287, no. 5454, pp. 836–839, 2000.

[19] S. Kim, E. Hawkes, K. Choy, M. Joldaz, J. Foleyz, and R.Wood, Micro artificial muscle fiber using niti spring for soft robotics, in Intelligent Robots and Systems, 2009. IROS 2009. IEEE/RSJ International Conference on. IEEE, 2009, pp. 2228-2234.

[20] S. Seok, C. D. Onal, K.-J. Cho, et al., Meshworm: a peristaltic soft robot with antagonistic nickel titanium coil actuators, IEEE/ASME Transactions on mechatronics, vol. 18, no. 5, pp. 1485–1497, 2013.

[21] Desmopan 2786A. https://www.tpu.covestro.com/en/Products/Desmopan/ProductList/201304281603/Desmopan-DP-2786A. Date accessed: 08.12.2018.

[22] M. Lefort-Tran, M. Bre, J. Ranck, and M. Pouphile, Euglena plasma membrane during normal and vitamin b12 starvation growth, Journal of cell science, vol. 41, no. 1, pp. 245-261, 1980.

[23] F. Ilievski, A. D. Mazzeo, R. F. Shepherd, X. Chen, and G. M. Whitesides, Soft robotics for chemists, Angewandte Chemie, vol. 123, no. 8, pp. 1930–1935, 2011.

[24] C. Cao, S. Burgess, and A. T. Conn, Flapping at resonance: Realization of an electroactive elastic thorax, in 2018 IEEE International Conference on Soft Robotics (RoboSoft). IEEE, 2018.